GATA 8(2): 41–58, 1991

IN SITU HYBRIDIZATION

Editor's Note: These articles are the second in a series on in situ hybridization edited by Glen A. Evans. Articles in the last issue of **GATA** covered DNA sequence mapping using electron microscopy and the analysis of genes and chromosomes by nonisotopic in situ hybridization.

Localizing DNA and RNA Within Nuclei and Chromosomes by Fluorescence in situ Hybridization

JOHN A. McNEIL,
CAROL VILLNAVE JOHNSON,
KENNETH C. CARTER,
ROBERT H. SINGER, and
JEANNE BENTLEY LAWRENCE

The enormous potential of in situ hybridization derives from the unique ability of this approach to directly couple cytological and molecular information. In recent years, there has been a surge of success in powerful new applications, resulting from methodologic advances that bring the practical capabilities of this technology closer to its theoretical potential. A major advance has been improvements that enable, with a high degree of reproducibility and efficiency, precise visualization of single sequences within individual metaphase and interphase cells. This has implications for gene mapping, the analysis of nuclear organization, clinical cytogenetics, virology, and studies of gene expression. This article discusses the current state of the art of fluorescence in situ hybridization, with emphasis on applications to human genetics, but including brief discussions on studies of nuclear DNA and RNA organization, and on applications to clinical genetics and virology. Although a review of all of the literature in this field is not possible here, many of the major contributions are summarized along with recent work from our laboratory.

From the University of Massachusetts Medical School, Department of Cell Biology, Worcester, Massachusetts, USA.

Address correspondence to Dr. Jeanne B. Lawrence, Department of Cell Biology, University of Massachusetts Medical School, 55 Lake Avenue North, Worcester, MA 01655, USA.

Received 3 October 1990; revised and accepted 2 January 1991.

History of Development

Many laboratories have contributed to the development and application of cytologic hybridization. Over the past 20 years, this technology has progressed from a laborious, time-consuming approach that detected abundant nucleic acid sequences with low resolution to an approach that enables relatively fast, highly precise, and sensitive localization of as little as one molecule per cell. The earliest phase of in situ hybridization technology relied on autoradiographic detection of abundant sequences, such as localization of DNA in amplified polytene chromosomes or highly reiterated sequences on metaphase chromosomes [1–3]. In 1981, two reports [4, 5] showed that it was possible to localize single sequences on metaphase chromosomes by autoradiography of ^{125}I- or ^{3}H-labeled probes using statistical analysis. This approach has since been used to map many genes and is still widely utilized, particularly for mapping of small (<1–2 kb) cDNA clones. Limitations are the relatively poor resolution, the fact that localization is not determined within a single cell but requires statistical analysis of many metaphases, and the time-consuming nature of autoradiography, which often requires several weeks.

To overcome these limitations, several laboratories had the foresight to pursue development of innovative nonradioisotopic detection techniques. Among the earliest were the use of antibodies to RNA–DNA hybrids and the initial reports of the biotin–avidin system to detect in situ hybridization using beads visualized by electron microscopy [6–8]. During the following decade, several approaches were described, including a method for direct labeling of fluorochromes to DNA probes [9, 10]; the incorporation of biotinylated dUTP into DNA probes [11] detected by antibiotin antibodies after hybridization to amplified polytene sequences [12]; the use of probes labeled with AAF (*N*-acetoxy-*N*-acetyl-2-aminofluorene) for detection of abundant sequences [13]; mercuration of probes [14, 15]; and sulfonation [16] or direct attachment of enzymes [17]. Most recently, a system using digoxygenin-labeled nucleotides detected by antibodies carrying fluorescent or enzymatic tags has been introduced (Boehringer Mannheim Biochemicals, Indianapolis, IN).

Labeled probes have most commonly been detected by fluorescent or enzymatic reporter molecules that recognize a modified probe. The enzy-

1050-3862/91/$03.50

matic detection methods, such as horseradish peroxidase and alkaline phosphatase, require extra steps to produce a visible product. However, they have advantages over fluorescence in that the reaction can be prolonged in order to amplify signals and the signals do not fade. Fluorescent tags, such as fluorescein or rhodamine, provide the highest resolution possible with the light microscope and can be adapted for multicolor labeling. Probes can also be detected with gold for electron microscopy (reviewed by Hamkalo [18]).

Over the last decade, different nonisotopic labeling techniques have been variously applied for detection of highly repeated DNA sequences or abundant mRNAs. For example, nonisotopic hybridization to satellite DNA was reported [19], amplified sequences were localized in polytene chromosomes [12, 20, 21], and clustered genes for ribosomal RNAs were detected on metaphase chromosomes [22, 23]. Although nonisotopic detection became more widely applied for highly represented sequences, the detection of single-copy genes during this period was done almost exclusively by autoradiography. There was some success in the nonisotopic detection of large (25–50 kb) unique sequences, using specialized procedures to amplify signals from either AAF-labeled probes with interference reflection microscopy [24] or biotin-labeled probes for mapping in *Caenorhabditis elegans* with image processing [25]. Perhaps due to apparent limitations of sensitivity and reproducibility in a growing number of nonisotopic methods, they were not widely adopted over radioactive techniques. Based on our analysis of various controls in initial unsuccessful attempts to use biotinylated probes for high-sensitivity detection, we concluded that difficulties in applying these techniques for single-sequence detection were not due to inherent limitations in sensitivity of the detectors, but rather arised because optimization of the total hybridization process had not been done. Based on this premise, we decided not to pursue alternative detection or amplification schemes, but rather to investigate systematically the various parameters important to the overall process, so as to identify and eliminate nonobvious sources of failure.

Characterization of Hybridization Parameters

The process of hybridization and detection of nucleic acids within cytological material is substantially more complicated than when nucleic acids are bound and hybridized on filters. Analytically, the steps of in situ hybridization can be divided into three main components: (a) *preservation* of target sequences in an accessible state within the biological material, which is critical for RNA but important for DNA as well; (b) *hybridization* of the probe to the target molecules with high efficiency and without substantial nonspecific adherence to biological material; and (c) *detection* of the probe with sufficient efficiency to give a detectable signal, with minimal nonspecific background. Failure of any one parameter in any of these components results in a lower signal–noise ratio and a loss of sensitivity.

Our work over several years emphasized quantitative characterization and optimization of hybridization and detection parameters, specifically for biotinated probes and fluorescence. For DNA detection, the goal was to detect single-copy sequences with hybridization efficiency high enough to provide consistent label on each sister chromatid and nonstatistical localization within individual cells. Although many laboratories had developed different protocols for in situ hybridization, it was difficult to know *a priori* which parameters were unnecessary or even destructive, and which were essential or required in order to improve results. To examine numerous variables and their interaction, an analytical approach was implemented that enabled rapid quantitation by liquid scintillation counting. The success of each of the three major components was individually quantitated, using ^{32}P–dCTP incorporated into the probe with dUTP–biotin (hybridization), ^{3}H–uridine incorporated into cellular RNA (preservation), and ^{125}I–avidin (detection). This was initially done for detection of cytoplasmic mRNAs and later for nuclear DNA [26–29]. Numerous variables tested had little effect. However, several key parameters were identified that improved results reproducibly. A few are summarized below to emphasize the essential and interrelated nature of what were a priori, nonobvious technical details. Other technical details can be found in the articles cited below and in the protocol at the end of this article.

Avidin Background

Testing numerous variables with ^{125}I–avidin, we found [27] that the widely reported nonspecific adherence of this protein to cytologic material could

be reduced ~90% simply by replacing phosphate-buffered saline, which we and others had employed previously [12, 30], with sodium citrate (4× SSC). The various chemically modified forms of avidin (streptavidin, avidin DH, and so on), developed in order to reduce its background, are unnecessary for single-copy detection, and in some cases give less intense signals than the original unmodified avidin (conjugated to fluorescein), which had been believed to stick nonspecifically to chromatin.

Kinetics

^{32}P-labeled total genomic DNA was used to evaluate hybridization kinetics. Standard autoradiographic gene mapping protocols called for long hybridization times (1–4 days) and low concentrations of probe (<1 ng/sample) [4, 5, 31]. The hybridization efficiency to single-copy sequences by these autoradiographic techniques is low. Our results showed that hybridization rises very sharply with time such that the reaction is one-third maximal in 10 min and essentially complete within 4 h (Figure 1A). Since hybridization of low copy sequences should continue to occur over a longer period, these results suggested that the rapid reannealing of chromosomal DNA may limit hybridization efficiency and should be competed with extremely high probe concentrations. However, higher probe concentrations had been generally considered prohibitive because of increased background [4, 5, 27]. Evaluation of signal and noise with increasing concentrations of ^{32}P-labeled probes repeatedly showed that hybridization still rises rapidly at 200 ng/coverslip (10 mg/ml), whereas background increases only very gradually, if other key variables are controlled (below). Hence, probe concentrations over 100 times greater than routinely used rendered much higher signal to noise ratios.

Probe Fragment Size

For in situ hybridization it cannot be assumed that two labeled preparations of the same probe, which have equivalent specific activities, will yield comparable results. In particular, the fragment size after labeling (commonly by nick translation) affects (a) the penetration of the probe into the cytological material, which is particularly important for tissue sections and intact cells [26, 32–34]; (b) the nonspecific adherence of the probe to cytological material [26, 28, 29, 35] (see Figure 1B). This is an extremely important parameter for in situ hybridization, especially with nonisotopic probes, and has been a major source of high background and failure in the past; and (c) the iterative detection of individual molecules (that is, if several probe fragments hybridize to a single target sequence, the signal will be distributed differently than the noise). This is most clearly observed for electron microscopic detection [36], but is also a significant factor in generating high signal–noise ratios with fluorescence.

Other Variables

Other parameters that significantly influenced the quality of results (often by preserving DNA) are: storing slides at −70°C and "hardening" by baking before denaturation; minimizing pretreatments prior to denaturation; omitting RNase A prior to hybridization; testing lots of formamide for neutral pH, correct melting point, and effectiveness for hybridization; and monitoring of time, temperature, and pH during denaturation. We found that autoclaving dextran sulphate further inhibits nonspecific sticking of probes. A variety of other previously described steps were tested and found to be unnecessary, such as extensive rinses, proteinase digestion, and acetic anhydride (useful only for some cell types with high endogeneous background).

High-Efficiency Fluorescence Hybridization

The results of these analyses were combined with elements of previous protocols [4, 5, 11] to show that a one-step fluorescein–avidin detection of biotinated probes, without amplification or image processing procedures, could detect single sequences of a few kb by standard fluorescence microscopy [29]. A critical aspect of this work was that the high hybridization efficiency and low background achieved allowed nonstatistical detection of single sequences in >90% of individual metaphase or interphase cells. Identical labeling of sister chromatids renders the relative position of the sequence along the chromosome length immediately obvious in just one metaphase (Figure 2A). The extremely high signal–noise ratio made it possible for the first time to localize *single* sequences within *interphase* nuclei. The results demonstrated a combination of high sensitivity,

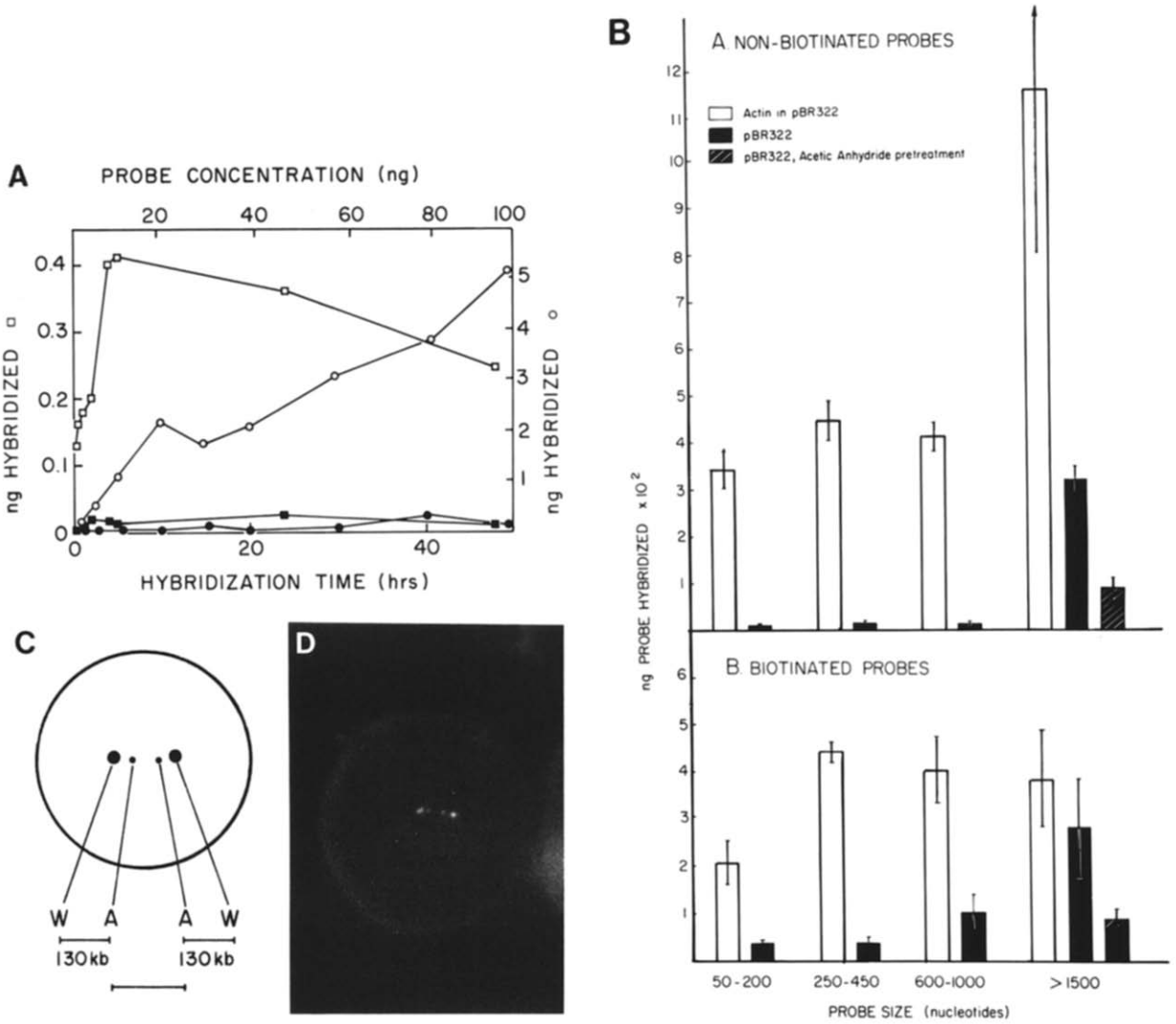

Figure 1. **A.** ^{32}P-labeled probe was hybridized to Hela cell chromosome preparations, and results quantitated by scintillation. Effect of time: open squares, total human DNA probe; closed squares, *Escherichia coli* control probe to assess background. Hybridization was for the times indicated at 37°C at a concentration of 4 ng/10 μl per sample. Each point represents the average of triplicate samples. Effect of concentration: the probe concentration is expressed as the nanogram of probe applied per sample in 10 μl of volume. Open circles, human DNA probe; and closed circles, *E. coli* control probe. Hybridization was at 37°C for 16 h and each point represents the average of duplicate samples. **B.** Results are from two experiments, each of which utilized duplicate samples to determine the effect of probe size on hybridization and background (bars indicate standard deviation). (A) Probes labeled with ^{32}P. (B) Probes labeled with biotin. Probe size was varied by changing DNase concentration in the nick translation. **C.** Diagram illustrating the interpretation of the pattern shown in **D,** and described in the text. **D.** Two probes (Bam H1 W and A), separated by 130 kb within the EBV genome, were hybridized simultaneously to Namalwa cell nuclei. The presence of four tightly clusetered spots of two different intensities (due to two different size target sequences) is observed in many G1 nuclei.

hybridization efficiency, signal–noise ratio, and resolution. This demonstrated the power of this technology for far-reaching applications in several areas.

This power was exemplified by analysis of EBV sequences in human lymphoma cells [29], which revealed a surprising degree of resolution between closely spaced sequences within decondensed interphase nuclei. This was first indicated by the presence of clearly paired fluorescent signals in the majority of interphase nuclei when only one chromosomal site was labeled. Further inspection indicated that in some metaphases, the signal on each sister chromatid could be resolved as two very close fluorescent spots (up to 0.4 μm apart). Larger G2 or tetraploid nuclei frequently had two "pairs" of spots. These results indicated the

presence of two closely integrated viral genomes, and coupled with evidence for only one set of viral–cell junction sequences [37], suggested that a duplication of viral and adjacent cellular sequences occurred during or after integration.

Further experiments demonstrated that, in fact, sequences at opposite ends of each individual EBV genome, separated by only 130 kb, could be simultaneously and individually visualized at interphase. As illustrated in Figure 1C and D, four spots were discernible in many interphase nuclei, two that were dimmer and two that were brighter, corresponding to the smaller A sequence (12 kb) and the larger W sequence (30 kb). From an analysis of cells in which the configuration of these four spots appeared in an extended linear array, it was surmised that the orientation of the two integrated EBV genomes was W–A–A–W, and that roughly 220 kb of cellular DNA separated them (Figure 1D). These results were corroborated by a second approach, whereby probes were hybridized separately, demonstrating a consistently smaller average distance between A–A signals than between W–W signals (significant at $p < 0.001$) and predicting a separation of 340 kb. These findings indicated that interphase analysis could be used to determine the order and approximate distance between tightly linked sequences, leading us to propose an approach to gene mapping by fluorescence hybridization termed "interphase chromatin mapping" [29].

Applicability for Human Gene Mapping

Figure 3 outlines a theoretical approach for rapidly evaluating the location and physical proximity of any two DNA segments using both metaphase analysis for unlinked or loosely linked sequences and interphase cells for tightly linked sequences. For simplicity, a one-label detection system is described. However, detection with two colors works well (see Figure 2 and Johnson et al. [38]) and three or more colors are possible [39]. The feasibility and limits of resolution for outcomes depicted in Figure 3 have been largely characterized in work described below. Figure 4 gives an overview of the range of distances approachable by established mapping techniques and compares these with fluorescence in situ techniques.

While nonstatistical sequence localization and high-resolution detection are essential for this scheme, the general applicability of this approach for genome mapping is greatly enhanced by the ability to use genomic probes containing repetitive DNA. Competition of "background" repetitive hybridization (see Figure 5C and D) using total genomic DNA has been used routinely for filter hybridization in many laboratories and was applied for in situ detection of whole chromosome libraries [40, 41]. It was important that this worked for single sequences, since successful use of genomic probes for autoradiography had not been demonstrated. Landegent et al. [42] first reported this approach for single cosmids detected with horseradish peroxidase and interference reflection microscopy using competition with Cot-1 DNA. For fluorescence detection, variations of this approach have been independently applied in a few laboratories, primarily for cosmids with >35-kb inserts [43, 44], and in our laboratory it has been routinely used for phage probes with 10-kb inserts [35, 45]. Figure 5 shows the impact of competition hybridization using a phage and cosmid probe, and illustrates a straightforward "double-label" with a single detection system, by targeting differently sized sequences. Two genes are rapidly detected within one metaphase, in contrast to autoradiographic or enzymatic techniques [46], which can provide excellent sensitivity, but generally require statistical analysis of many metaphases to localize a single gene, most commonly with lower resolution.

Approaches to Metaphase Mapping

The ability to visualize single sequences within individual chromosomes makes it possible to describe sequence location in terms of relative position along the length of unbanded chromosomes. Lichter et al. [44] demonstrated the ability to order numerous chromosome-11 cosmids based on measurements of signal position relative to total chromosome length from digital images. This is clearly a valuable approach to determine approximate localization or relative order.

Because the entire genetic map is currently expressed in terms of cytogenetic bands, it is important that fluorescence mapping can be coupled with banding and that the precision of mapping by measurement versus banding be directly evaluated. In collaborative efforts, we have adapted various cytogenetic banding techniques, including G, Q, and replication, for fluorescence mapping of several human genes [45, 47, 48]. Other groups have also reported successful coupling with R-banding [49, 50].

Direct comparison between banding versus measurement previously indicated [35] that fluorescence mapping on either banded or unbanded chromosomes provides improved precision over autoradiography [35, 45]. However, banding provided the most accurate and precise placement (Figure 6A and B), with the added advantage of being independent of chromosome condensation. The banding results narrow the localization to a region encompassing ~5–7 megabases of DNA. Restricting measurements to highly elongated chromosomes (see bar in Figure 6B) decreases the range significantly. However, this approach is still less accurate than banding. A similar discrepancy in position was observed for other genes, such as dystrophin, known by several criteria to map at Xp21.2 (Figure 6D and Davies et al. [51]). For five different genes for which these approaches were directly compared, there was precise agreement between bands and measure-

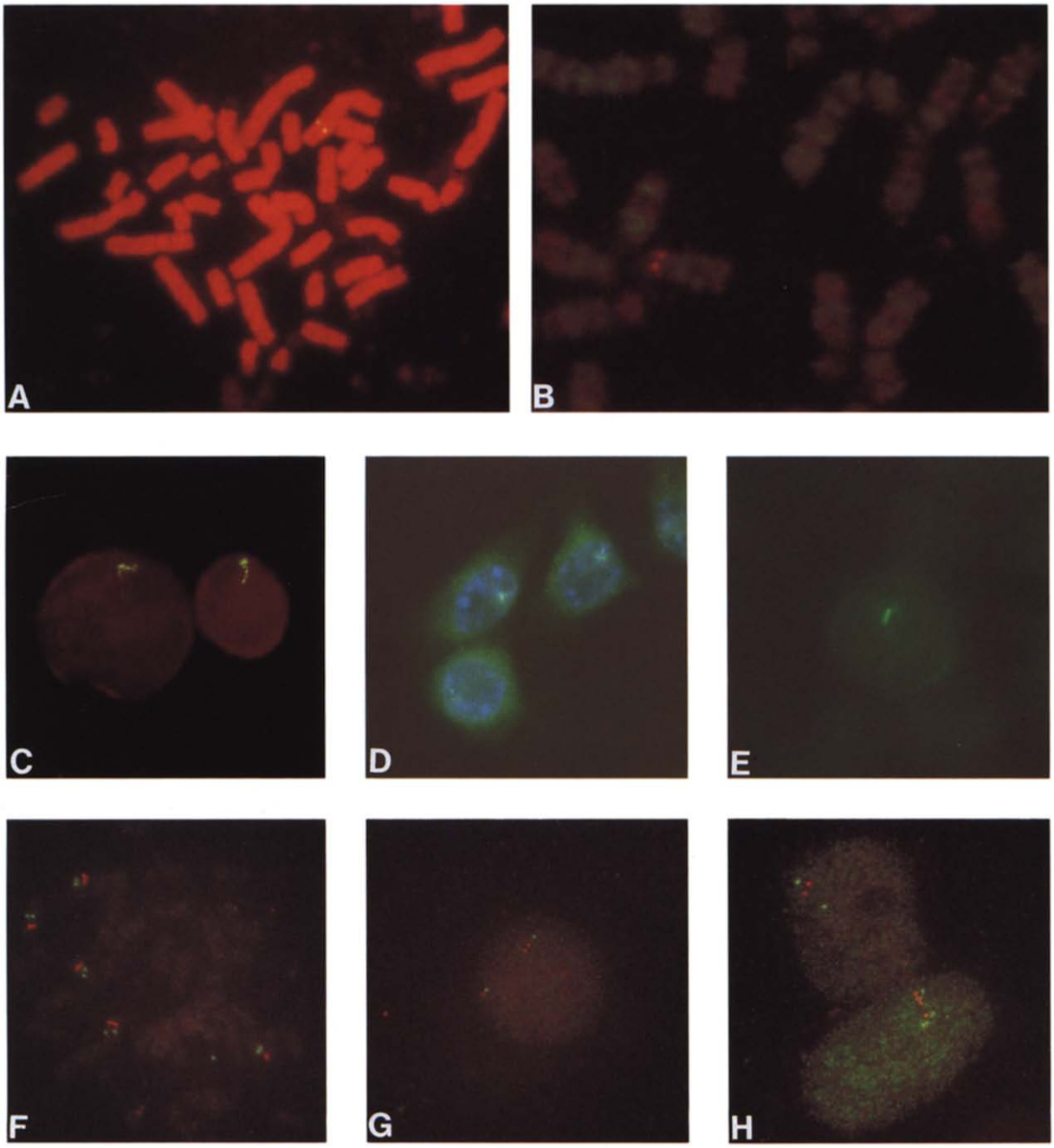

ments in two cases and a shift in apparent band position in three. This inaccuracy is largely due to the fact that placement of bands on ideograms is not based strictly on measurement, because relative band position varies with condensation and other technical factors [52].

Technical considerations for several banding techniques have now been worked out (see [53] for further details). Giemsa–trypsin produces high-quality banding patterns. However, simultaneous visualization of bands and fluorescent signal is not possible, due to the high reflectivity of Giemsa stain. As illustrated in Figure 6C, banding can be photographed prior to hybridization, and then slides destained in 3:1 methanol–acetic acid before hybridization and rephotographing. Accurate placement of signal is dependent on proper alignment of photographs.

Q-type bands can be obtained by DAPI staining, which is simple, reproducible, and does not interfere with hybridization signal, but can require a second fluorescence filter and two photo-

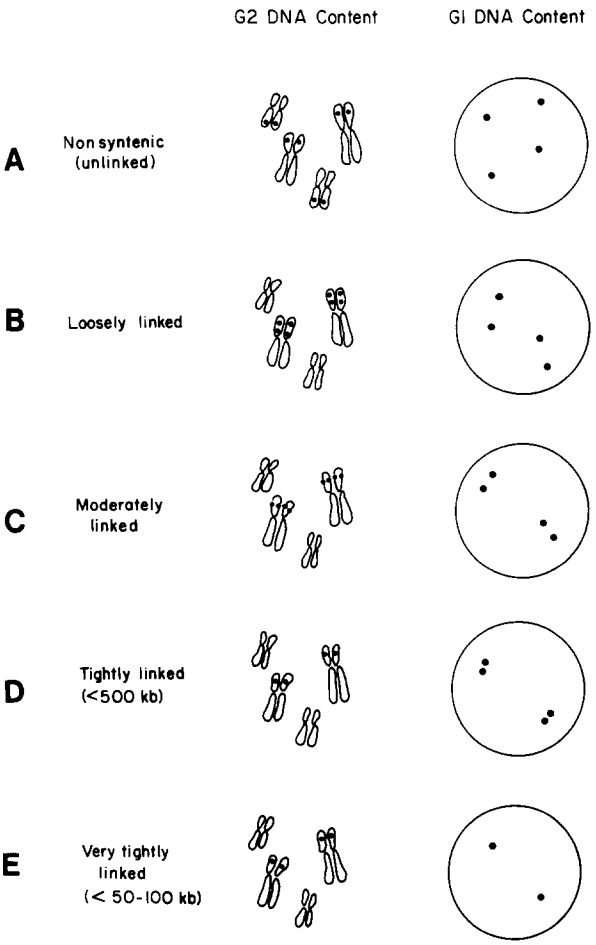

Figure 3. Schematic outline of gene mapping in interphase and metaphase cells. Simultaneous hybridization of two probes to cytogenetic preparations containing both metaphase and interphase cells is visualized by routine fluorescence microscopy. **A.** Unlinked or nonsyntenic sequences are readily resolved at both metaphase and interphase. Metaphase cells have a G2 DNA content and, hence, have twice as many signals as G1 interphase cells due to the identical labeling of sister chromatids. **B.** Loosely linked sequences will be resolvable along the chromosome length and show only a distant pairing within interphase nuclei. **C.** As sequences become closer, they will no longer be resolvable along the chromosome length, but may be separable across the width. **D.** Sequences difficult or impossible to resolve at metaphase will still be clearly visualized as closely paired signals within decondensed interphase nuclei, with the distance between paired signals proportional to DNA distance. **E.** The closest physical linkage would be represented by sequences too close to resolve at either metaphase or interphase.

Figure 2. **A.** The localization of this 18-kb sequence of the integrated EBV genome is readily apparent due to the identical sister chromatid labeling of a specific position on Chr. 1. Chromosomes are labeled with propidium iodide and probe detected with fluorescein–avidin. **B.** Simultaneous visualization of hybridization signals with G-bands identified by BrdU incorporation. Use of a dual-band filter allows the fluorescein-labeled bands to be photographed with the rhodamine hybridization signal (for the Blast-1 gene on chromosome 1) with a single photographic exposure and no optical shift. One labeled chromosome 1 is left of center, and the other is in the upper right. **C.** Primary nuclear transcripts from a latent EBV genome show a very localized "tracklike" distribution. These formations of nuclear RNA become especially elongated in cytogenetic preparations, as shown here. Several hundred copies of the RNA are detected [78]. **D.** A highly focal distribution of primary transcripts is also seen from expression of the neu–proto-oncogene after transfection into mouse 3T3 cells in which it is highly expressed [78]. Paraformaldehyde intact cells are shown, in which the neu sequences present in the cytoplasm are also detected. Blue is DAPI DNA staining and green is hybridization signal detected by fluorescein–avidin. **E.** A single focus or small "track" of newly transcribed HIV RNA is apparent in the nucleus of most infected cells before the cytoplasmic fluorescence becomes apparent [80]. Against a background of many unstained negative cells, a single expressing cell can be detected only 12 h after infection, in paraformaldehyde lymphocytes. **F.** Two-color labeling with biotin and digoxigenin-labeled probes allows the relative localization of three probes to be determined. In this polyploid metaphase, two probes were detected in red and one in green. The two red probes are found to be so close (<1 Mb) that they appear at one site on the metaphase chromosome, whereas the green probe is more distant (see **G**). **G.** In the interphase nucleus the order of three probes can be assessed, and in this photograph the two red probes separated by <1 Mb could be resolved and ordered with respect to the green probe. The further apart the probes are, the greater the variation seen in the order observed at interphase due to the three-dimensional folding of the chromatin fiber. Hence, statistical analysis of the frequency of specific orders is necessary in many cases. **H.** Two other potential sources of confusion in the interpretation of results are illustrated here by the two-color detection of two probes separated by several Mb on chromosome 17. First, in the upper cell the two homologs are close enough together to make it difficult to discern which pair of red and green signals derives from the same homolog. Second, even in this population of confluency-arrested G1 fibroblasts, there are still G2/S phase cells that have extra signals due to the presence of replicated sequences.

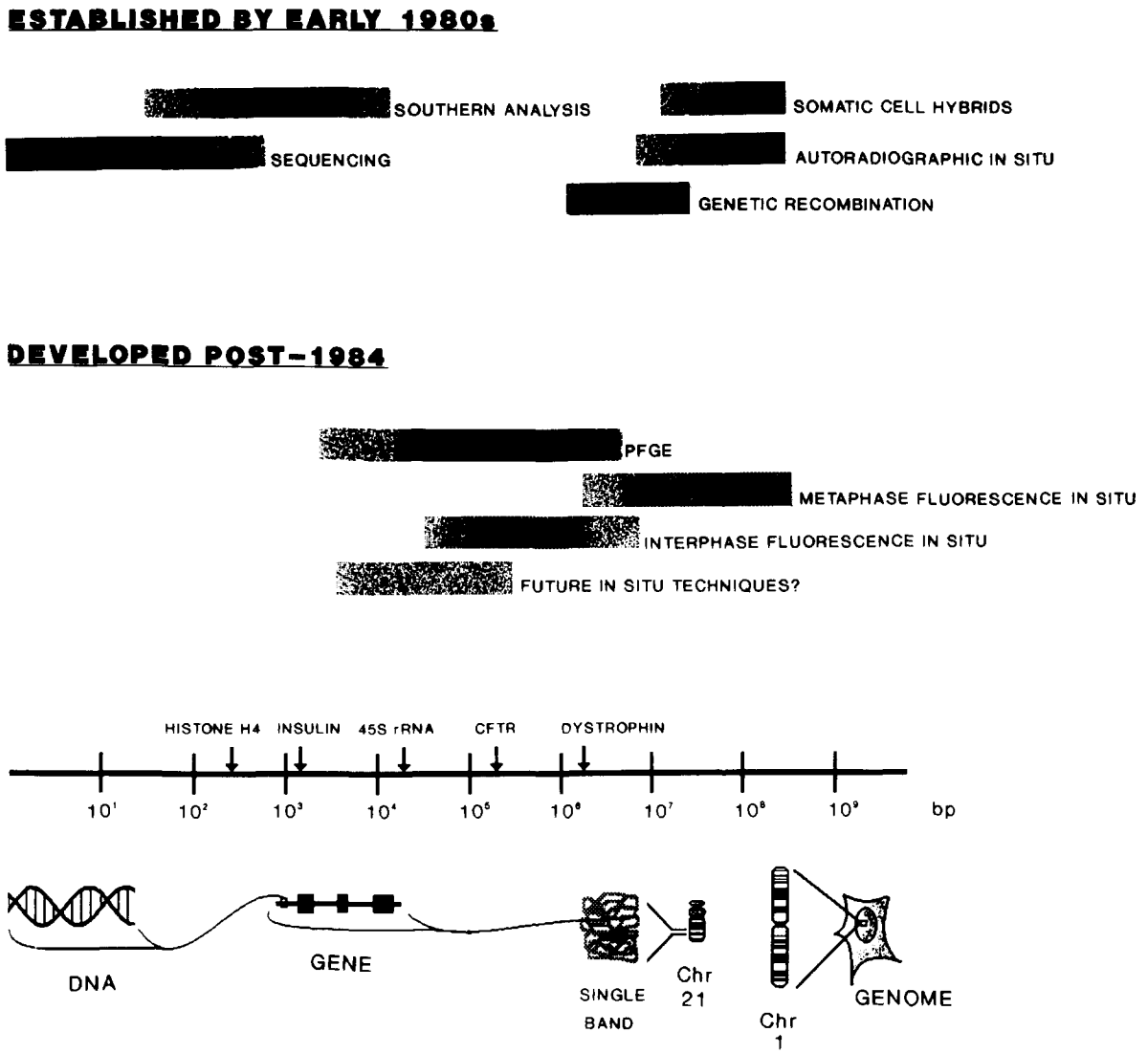

Figure 4. Comparison of the range of DNA distances over which different gene-mapping techniques can be utilized. Lighter regions of each bar indicate a range for which the method has variable utility. Techniques are displayed from top to bottom in approximate chronological order. Grey bars indicate fluorescence in situ hybridization approaches, black bars indicate other techniques. PFGE, pulsed-field gel electrophoresis; and CFTR, cystic fibrosis transmembrane regulator.

graphs [48, 53]. The contrast of bands is improved by incorporation of bromodeoxyuridine (BrdU) into late-replicating DNA. Recent technical developments will provide optics that enable visualization of DAPI with other fluorochromes (unpublished results).

BrdU incorporation into late-replicating G-bands [54] can be detected by the addition of a fluoresceinated antibody to the probe detection step, providing a rapid and convenient means of chromosome identification (Figure 3A and [35]). The significant advantage is that bands and signals are viewed and photographed using a single filter set that enables simultaneous visualization of fluorescein and Texas red [38]. This circumvents registration problems associated with superimposition, alignment, or double exposures. Commercially available anti-BrdU antibodies (Becton-Dickinson, Partec) require that the DNA be single-stranded. However, after hybridization there is enough denatured genomic DNA to produce an excellent banding pattern [35, 55].

Finally, hybridization to specific repetitive elements can be exploited for chromosome identification [56], since LINE sequences are concentrated in the R-bands and Alu in the G-bands [57, 58].

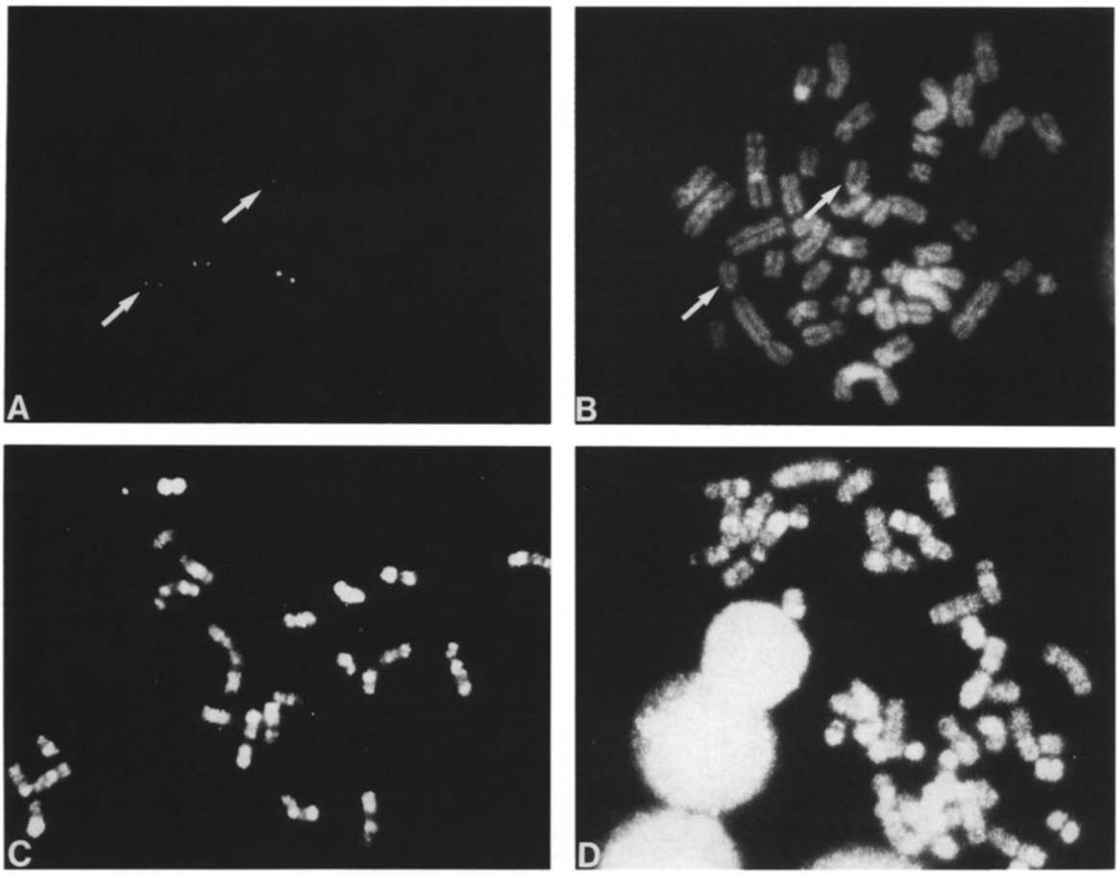

Figure 5. Simultaneous visualization of two nonsyntenic genomic probes using competition hybridization and intensity double labeling. **A.** Simultaneous hybridization to the neu-proto-oncogene (erb-B2) [60] and cardiac myosin heavy chain gene [93] in the presence of 0.15 mg/ml of DNase-digested unlabeled total human placenta DNA. Repetitive hybridixation (see **C** and **D**) is almost entirely eliminated, allowing the single-copy component of the targets to be detected. The phage and cosmid probes give different signal intensities due to the smaller (12 kb) target size of the MHC probe (arrows) compared to the neu cosmid (35 kb). **B.** DAPI total DNA staining of chromosomes shown in **A.** The positions of the dimmer MHC signals (see **A**) are indicated with arrows. The cardiac MHC gene previously localized to chromosome 14 [93], can be regionally localized just beneath the centromere on the long arm of this chromosome, and the neu gene has been previously localized to chromosome 17. **C** and **D.** Hybridization of each genomic probe separately in the absence of unlabeled excess human genomic DNA results in hybridization to repetitive DNA dispersed throughout the genome. The "single-copy" sequence is masked by the repetitive hybridization, which produces light and dark regions or "bands" on the chromosomes that vary depending on the particular repetitive elements present in the probe. Residual repetitive hybridization can be useful for visualization of chromosome morphology and aids in chromosome identification.

Limits of Metaphase Mapping

A key question concerns the point at which sequences become too close to be ordered by chromosomal hybridization. A distinction must be made between resolution of sequences along the chromosomal length, which is useful for ordering, and resolution across the width, which is generally not. To address whether metaphase mapping can be effective in the 1-Mb range, we used the large, well-characterized human dystrophin gene [59] as a test system. This analysis [35] demonstrated that sequences separated by 1.1 Mb were resolvable across the *width* of each chromatid, but only on more condensed chromosomes (Figure 7C and D). On less condensed prometaphase chromosomes, the two signals coalesced into one. Analysis of metaphase hybridizations representing distances from 125 kb to 1.1 Mb indicated a very variable occurrence and configuration of "doublet" signals on contracted chromosomes with probes separated by a few hundred kilobases or more. Even with two-color detection systems, the order of dystrophin sequences separated by 750 kb was not apparent. Hence, metaphase mapping is apparently limited by the fact that the chromosome width of even less condensed chromosomes encompasses substantial quantities of highly packaged DNA. Chromosome mapping

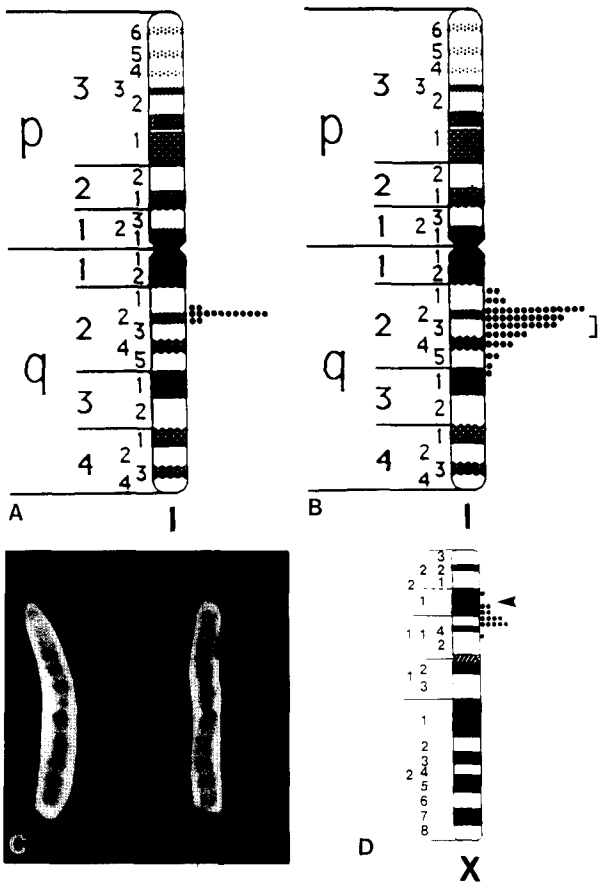

Figure 6. Comparison of metaphase gene localization methods. **A.** Fluorescence detection of in situ hybridization on G-banded chromosomes. Metaphase figures were Giemsa/trypsin banded, photographed, and then rephotographed after fluorescein–avidin detection of hybridization with Blast-1 genomic phage probes. The total chromosome morphology was visible with fluorescein staining due to residual hybridization to repetitive DNA, allowing precise alignment on a grid of the photographs of Giemsa-stained and fluorescein-stained chromosomes, using centromeres and telomeres as reference points. Although the prior trypsin banding treatment does weaken hybridization signal slightly, this 20-kb target was still clearly detectable. **B.** Fluorescent detection on unbanded chromosomes. Signals were localized by measurement along the chromosome length. To correct for differential chromosome condensation each data point was expressed as the ratio: (distance from telomere to signal)/(total chromosome length). **C.** Trypsin G-banded chromosomes and the corresponding fluorescent signal for the Blast-1 gene, as described in **B. D.** Ideogram of localization of the dystrophin gene by measurement on unbanded chromosomes. The well-characterized gene is known to be located at Xp21.2 (see arrow). However, measurements place it slightly lower.

may be most practical for sequences separated by a few Mb or more. For example, hybridization to sequences separated by several centimorgans (roughly several megabases) can barely be resolved and ordered along the length of longer chromosomes (Figure 7B and White et al. [60]).

Interphase Mapping

Metaphase mapping is important for rapid localization to a chromosome region, but complete mapping of the human genome will largely involve analysis of sequences not far enough apart to be ordered at metaphase. The demonstration that very tightly linked DNA sequences could be resolved by light microscopy within interphase nuclei [29] indicated that closely spaced genes are much further apart than predicted by the total condensation of nuclear DNA of 1:1000 or greater [61]. The order and distance between integrated viral sequences was evaluated in two different ways, the agreement of which provided validity to what was then a totally unproven approach: (a) the order of sequences was surmised by the arrangement of four signals within individual nuclei using intensity "double-label"; and (b) the average distance between pairs of signals with one probe was compared to that with the other probe, based on analysis of many nuclei.

Because the DNA strand must fold in a complex three-dimensional configuration in order to package its enormous length into a chromosome or nucleus, the use of interphase mapping must remain somewhat circumspect until the relationship between interphase distance and linear DNA distance is more fully characterized (for example, for different distances, areas of the genome, cell types, or preparations). Two reports have thus far provided further evidence in support of this approach. Trask et al. [43] first reported an approximately linear correlation between interphase distance and known DNA distance for sequences separated by up to 250 kb in the dfhr locus of a chinese hamster cell line. The correlation was sufficient to accurately predict the order of cosmid sequences in that range. We characterized this relationship for normal human sequences, in diploid cells, up to a range of 1 Mb, where loops in the chromatin fiber [61, 62] might be most likely to distort this relationship. For this purpose, our work utilized the large, well-characterized dystrophin gene [59]. As expected for X-chromosome sequences, single dystrophin probe hybridization to male lymphocytes produced a single hybridization signal, with the important exception of nuclei shown to be in G2, which contained two very closely spaced signals representing replicated DNA [35]. In contrast, targeting two sites separated by 100 kb–1 Mb produced two precise, closely spaced signals in

the majority of nuclei (Figure 7E and F). Importantly, the difference between smaller (300 and 375 kb) and larger (675 and 750 kb) distances was discernible by brief microscopic examination.

Despite a normally distributed intercell variation (Figure 8, inset), average interphase distances in the 1-Mb range show a strong correlation with DNA distance, which approximates linearity (Figure 8). This represents a linear region of a curve with a decreasing slope, since sequences separated by 6 centimorgans (roughly 6 Mb) were 2.8 μm apart, and sequences 70 Mb apart were only about 6 μm apart at interphase. The correlation is sufficient to allow ordering of distances differing by 75–150 kb in the 1-Mb range [35] and possibly as little as 40–50 kb for smaller distances [43]. Although the relationship between interphase distance and DNA distance may vary with the particular region of the genome studied, it is encouraging that for the three different systems studied thus far (EBV in human lymphoma cells [29], dfhr sequences in chinese hamster [43], and dystrophin gene sequences in normal diploid human lymphocytes [35], similar condensations are observed at a given distance. As shown in Figure 8, the 1-Mb intragenic distance for dystrophin measured in two different cell types (PBLs and G1 arrested W138 fibroblasts) yielded remarkably close interphase distances. The lower limit of interphase resolution is clearly <100 kb for dystrophin sequences, and several observations indicate that sequences separated by ~25 kb are just at the limit of resolution of fluorescence microscopy (0.1–0.2 μm apart [35, 43]).

These results clearly indicate that interphase mapping is useful for ordering. Although the use of two-color detection (Figure 2) can increase the speed of data acquisition, it should also be cautioned that as sequences become further apart, the interpretation of order at interphase becomes increasingly subjective and must be based on analysis of many cells. It is essential to confirm that G2/S phase or tetraploid cells have been eliminated (see Figure 2). As yet, estimates of actual DNA distance from interphase distance should be considered very approximate, since chromatin condensation may vary substantially. Hence, the correlation depicted in Figure 8 provides at best a crude standard.

As summarized in Figure 3, the combination of interphase and metaphase fluorescence hybridization extends across a broad range of physical distances. Using this cytological procedure one can visually resolve DNA sequences 1–2 orders of magnitude closer than by genetic recombination analysis, autoradiographic in situ hybridization, or standard somatic cell hybridization. Using two-color detection with dual-band filters, the amount of data obtained from each sample may be enhanced, by allowing easy assessment of the order of clones. This rapid and straightforward approach may provide a valuable complement or alternative to other fine-structure mapping techniques, particularly pulsed-field gel electrophoresis. For example, a combination of metaphase and interphase analysis might allow a relatively rapid means of ordering a series of overlapping cosmids or YAC clones, or of screening clones for those close to a marker for a disease gene, or lying between two flanking markers for a sequence of interest.

Nuclear Organization and RNA Localization

Efforts to describe and understand the organization of complex genomes completely will ultimately include investigations into the three-dimensional organization of the nucleus in its functional state at interphase. The nuclear genome is not simply a linear structure, hence it is important to provide not only a detailed linear map and sequence, but to seek concomitantly the basic principles and functional significance of its total in vivo organization. High-resolution in situ hybridization provides a powerful approach for the investigation of higher-level chromatin packaging, localization of specific genes or their primary transcripts within the nucleus, and potential changes in nuclear organization with different functional states.

In recent years, much has been learned about the nucleosome structure of chromatin (reviewed by Georgiev et al. [63] and Weisbrod [64]), but, as yet, much less is known about higher-level organization [55, 65]. Since first proposed [66], a three-dimensional ordering of chromatin in the interphase nucleus has been suggested by a variety of cytological observations [67–76]. It has been suggested that active genes are localized near the nuclear periphery [77]. However, the detailed investigation of nuclear organization is at an early stage and has been restricted primarily to repetitive sequences or nuclear landmarks, such as the nucleolus. Much more refined analysis can now be done, since the tools are available for localiza-

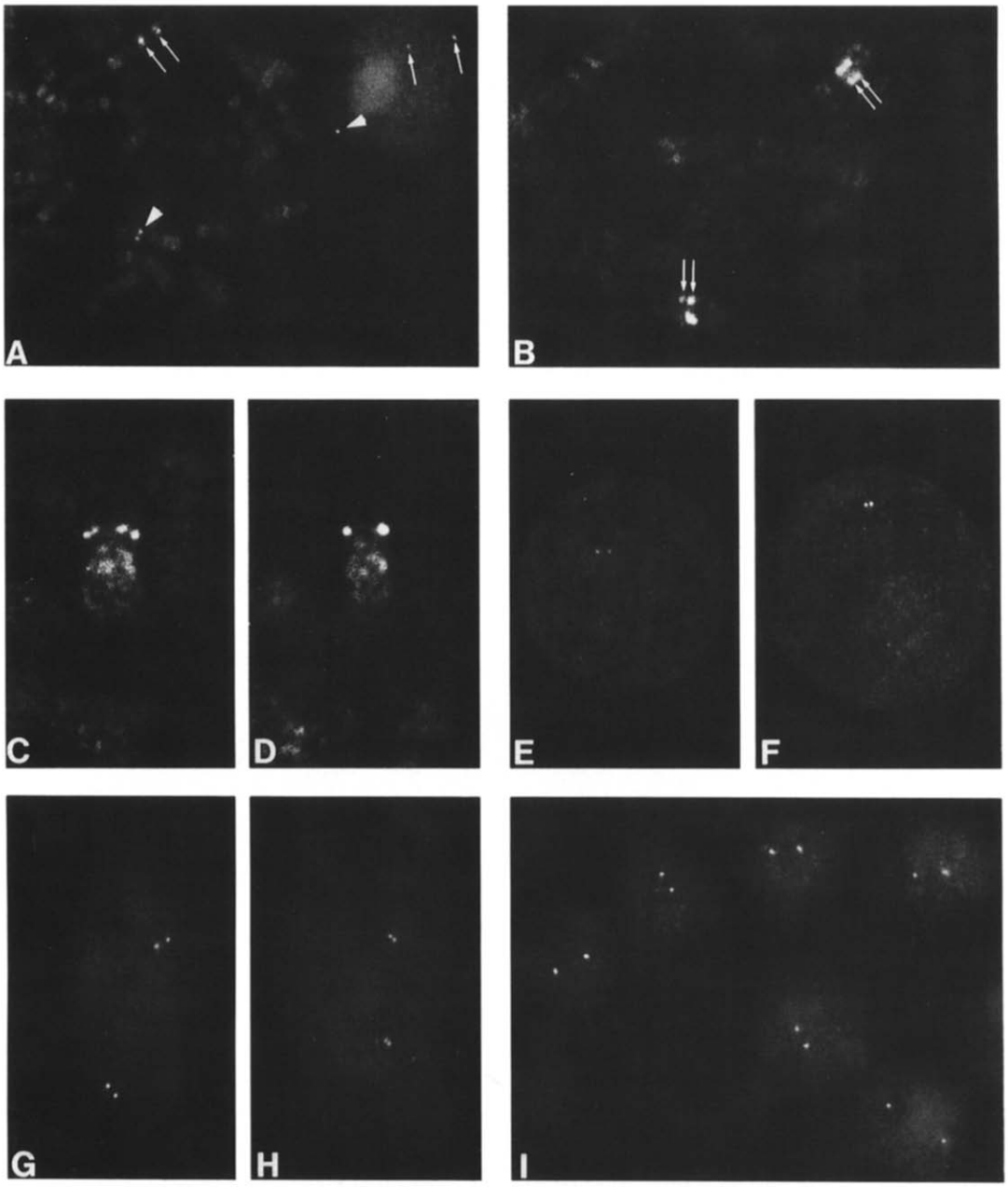

tion of specific single-copy genes. This type of analysis, for instance, revealed that the EBV genome is confined to an inner sphere of the nucleus representing only 50% of the volume, strongly indicating a sequence-specific higher-level order within interphase chromatin [29]. Simultaneous visualization of closely linked sequences has provided other important clues to the organization and packaging of DNA, such as (a) the condensation for 125 kb of a normal human gene is ~1:73; (b) sequences up to 1 Mb apart are often separated across the width of metaphase chromosomes; (c) replicated "sister chromatin" genes are closely aligned within S/G2 cells; and (d), for several genes studied, homologous sequences are not somatically paired [35]. Implications of these findings for nuclear organization are detailed elsewhere [35, 53].

Much of our methodologic work (see above) has been directed toward preserving and sensitively detecting specific RNAs as well as DNA. Studies of nuclear RNA can provide important insights into the overall structure of the nucleus and the processing and transport of primary tran-

Figure 7. Results of fluorescence in situ hybridization, presented in order of decreasing physical distance. **A.** Hybridization of a chromosome-1 sequence to cytogenetic preparations of the Namalwa cell line, illustrating how a cytogenetic abnormality is evidenced by the nonidentical labeling of sister homologs. Based on an estimate of 250 Mb for the DNA content of chromosome 1, the duplicated sequences are separated by 70 Mb of DNA. Note that three signals, rather than two, are observed within the interphase nucleus. The duplicated sequences from one homolog are ~5 μm apart at interphase. **B.** Simultaneous hybridization to neu (erb-B2) and nerve growth factor receptor cosmid clones, which are loosely linked and frequently resolvable along the length of less condensed metaphase chromosomes. These sequences have been localized to separate bands (17 q11.2-q12 and 17 q21.3-q23, respectively) and are ~10 centimorgans apart (roughly 10 Mb) based on their respective proximity to the NF1 locus [60]. **C** and **D.** Resolution of sequences across the width of metaphase chromosomes. After simultaneous hybridization of two probes separated by more than 500 kb, two discrete signals on either side of the chromatid axis are frequently obsrved (**C**). In contrast, hybridizations with probes separated by smaller distances generally results in one fluorescent signal on each sister chromatid (**D**), as does single-probe hybridization. The distance between paired signals on each chromatid is variable and related to the degree of chromosome condensation. **E.** Interphase nucleus of male peripheral blood lymphocytes showing hybridization to two sequences within the dystrophin gene separated by ~1050 kb. **F.** Same as in **E**, except sequences were separated by 375 kb. **G** and **H.** High-resolution of sequences within interphase nuclei of intact, paraformaldehyde-fixed W138 fibroblasts (derived from a female). **G.** Dystrophin sequences separated by 650 kb are clearly separated, resolvable in ~90% of nuclei. **H.** Very closely paired signals are frequently (~20% in W138) resolvable after hybridization with the a-cardiac MHC probe, which is homologous to both the a and MHC genes on chromosome 14 [93]. **I.** Lower magnification view of hybridization to two overlapping cosmid probes for the neu–proto-oncogene (erb-B2). The probes produce one large signal for each Chr. 17 homolog, with no evidence of closely spaced pairs. These sequences are generally localized in the internal region of lymphocyte nuclei, and hence illustrate the maximal degree of homologous pairing of any sequences tested thus far.

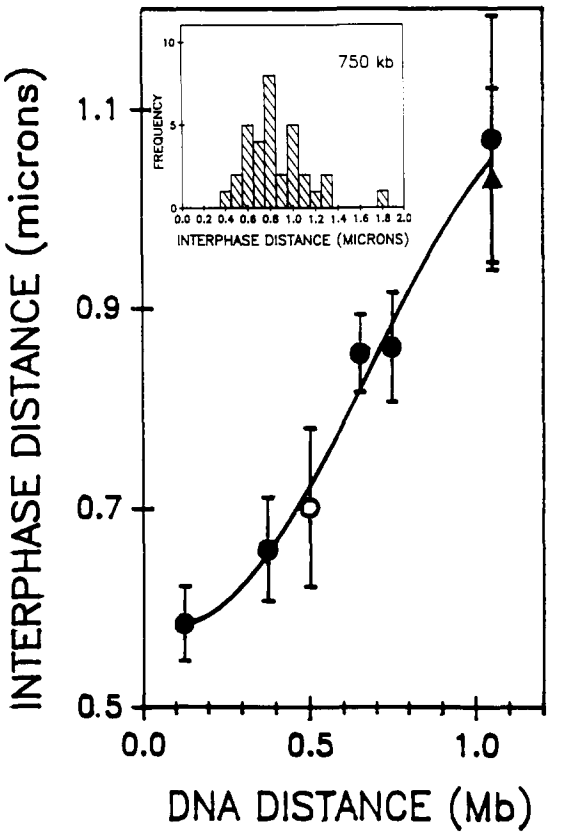

Figure 8. Relationship between DNA distance and interphase distance of dystrophin sequences. Symbols indicate the average SEM. Points were determined in normal peripheral blood lymphocytes (PBLs), except the 1-Mb distance was determined in both PBLs (circles) and in primary G1-arrested W138 fibroblasts (triangle). Solid symbols indicate larger data sets (35–60 nuclei) and open circles indicate smaller data sets (16–20 nuclei). The curve was derived by third order regression and is presented for emphasis. Although the relationship in this size range appears generally linear, the larger picture would predict a curve with gradually decreasing slope (see text and [35]). Insert shows the distribution of measurements taken from signals separated by 750 kb.

scripts. For example, high-resolution visualization of specific viral RNAs has revealed highly localized, often elongated "tracks" of nuclear RNA that contain up to several hundred copies of the mRNA [78]. These results suggest a highly structured nuclear interior in which RNA is not freely diffusing. Coupling of biochemical fractionation procedures with in situ hybridization has further elucidated the association of these RNA formations with the nonchromatin nuclear substructure or matrix [79]. Detection of primary nuclear transcripts has been shown for neu-oncogene sequences in transfected cells [78], for HIV RNA from single genomes [80], and for endogeneous RNAs of individual genes (J. B. Lawrence, C. V. Johnson, Y. Xing, unpublished results). This enables gene-specific transcriptional activity within a single cell to be elevated. Other potential applications include investigating genetic diseases that may result from RNA-processing defects and screening cloned genomic DNAs to find expressed sequences.

Potential Applications for Analysis of Cytogenetic Aberrations

The speed, convenience, and precision of nonisotopic probe-labeling techniques makes it feasible to apply cytologic hybridization to the characterization of cytogenetic aberrations for both research and diagnostic purposes. The current status of this technology makes possible a new area of "molecular cytogenetics" whereby standard karyotypic analysis is directly coupled with molecular biology. The field of cytogenetics has

been limited to the analysis of relatively gross chromosomal aberrations based on banding patterns, deviations containing 10 Mb or more of DNA. Using cytologic hybridization, it is now possible to detect just a few kb of deleted or misplaced DNA, since aberrations resulting in the nonidentical labeling of homologous chromosomes are readily apparent.

Several groups recognized the potential of using whole chromosome libraries on specific probe subsets to detect trisomies, monosomies, and translocations. The advantage of in situ hybridization for this purpose is that analysis can be done by interphase cytogenetics, as described by Cremer et al. [81] for trisomy 18. This approach has also been applied for the detection of trisomy 21 [41, 82] and is applicable to sex chromosome abnormalities as well. The use of chromosome "painting" will be more fully described elsewhere [83].

The success of single-copy techniques now renders many duplications (Figure 7A) and deletions [84] immediately apparent. This may be particularly important in the diagnosis of carriers, since quantitation of gene dosage is very difficult by Southern blots. In contrast, the presence of a deletion in the dystrophin gene in female carriers is unambiguous by in situ hybridization, since it results in one labeled homolog and one unlabeled homolog in interphase and metaphase cells [85]. The ability to detect heterozygous deletions in interphase cells has particularly important potential for detection of tumor suppressor genes for diagnostic or prognostic purposes. These techniques may also facilitate the identification of such genes [48].

Application to Viral Detection and Expression

While our initial work using the EBV model system [25] provided the basis for developing gene mapping methodology (see above), it also had considerable implications for virologic analysis at the single-cell level. The work demonstrated that in the cells studied there was a duplication of a portion of chromosome 1 containing the viral sequences and several hundred kilobases of cellular DNA. The ability to investigate integration in a single cell may eventually reveal aspects of the mechanism of integration or the relation to disease states hitherto undefined. We have recently used this approach in work showing that EBV integration is much more common in certain cell types than previously believed [86]. As illustrated in Figure 9B, individual episomes could be visualized, and were distinct from integrated genomes, which consistently label both sister chromatids. Whether herpes viruses need to be integrated or can remain episomal and still transform cells can be more rigorously addressed by this approach, as could the question of how episomes replicate and become distributed to daughter cells.

Expression of viral genes can be monitored in single cells as well. When the target cells or tissues are not denatured, only RNA will hybridize. This approach provides evidence for the timing and expression of genes during the viral life cycle. In cells containing many episomal EBV genomes, numerous discrete foci of viral RNA were observed [79, 80], indicating that many or all of the episomal genomes are transcriptionally active.

This technology has been applied to the detection of HIV-infected cells [80, 87]. Within hours after infection of lymphocytes, a focus composed of newly formed RNA is apparent in the nucleus (Figure 2F), suggesting the activity of a single genome. A singular focus was also observed in a cell line known to carry a single integrated copy of HIV, and the same singular focus can be seen in cells of lymphocytes from patients, suggesting the presence of just one viral genome early in infection. Use of this technology also allowed a single integrated HIV genome to be visualized on one homolog of a D-group chromosome in the 8E5 cell line (Figure 9A).

Specialized Microscopic Techniques

An important recent advance for standard fluorescence microscopy is development of dual-band filter sets, which enable simultaneous visualization of two fluorochromes, as illustrated in Figure 2. This enables the order of three single-copy probes to be determined using two-color detection. Simple double- or triple-exposure photographs, as described for multiple-color labeling of repeated sequences [39], are of no use in the analysis of closely spaced probes, because the image shift from one filter set to another is sufficient to cause loss of precise positional information. Accurate registration of images using computer-assisted image processing is difficult and often requires use of a fiduciary marker that appears in both pictures [44]. The development of relatively

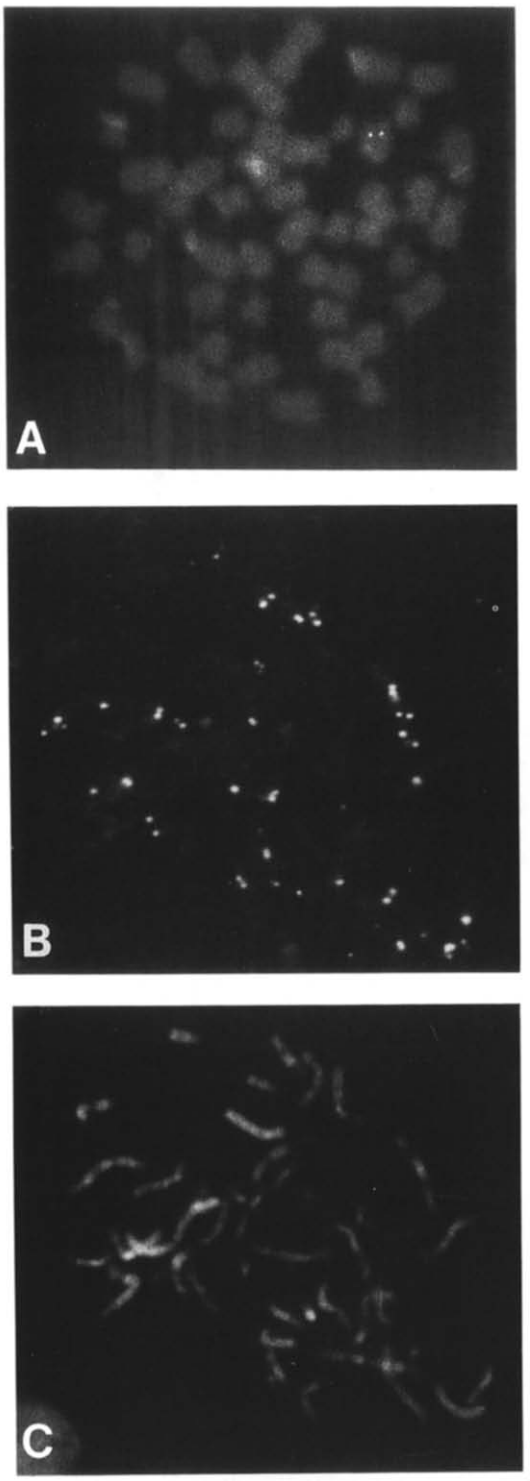

Figure 9. Detection of episomal and integrated viral sequences. **A.** Localization of a single HIV integrated sequence detected on both sister chromatids [80]. **B** and **C.** Detection of episomal EBV genome in a cell line carrying numerous nonintegrated viral genomes [86]. **B.** Hybridization signal. **C.** DAPI staining of metaphase in **B.**

inexpensive double-label filter sets helps avoid this, and further details are presented elsewhere [38].

Advances in digital image capturing, processing, analysis, and storage offer some important advantages for certain applications, as reviewed elsewhere in this volume [56]. Direct visualization of biotinated probes below 3 kb is difficult using a one-step fluorescein–avidin detection, although brighter signals can be obtained by antibody amplification for biotinated probes [88]. (We have found probes of 2 kb to be readily detectable using digoxygenin labeling.) As illustrated in Figure 10, however, a digital image of hard-to-see signals (2 kb) can be greatly enhanced to make the signal more obvious. Localization of sequences of <4 kb using an ISIT camera and computerized image registration has been reported [23, 89]. Image processing and optical sectioning can be essential for studying the three-dimensional organization of the interphase nucleus (see, for example, Manuelidis [90] and Paddy et al. [91]). Other very important developments are the use of confocal microscopy and flow cytometry for rapid quantitation of RNA or DNA content (reviewed by Gray et al. [83] and Bauman et al. [92]).

General Method for Detection of Single-Copy DNA

Reagent quality is a critical factor for successful detection of single-copy DNA sequences, particularly of the formamide, labeled nucleotides, and water. Protocols should be adhered to precisely, or modified carefully, because seemingly innocuous changes can be detrimental.

Cytogenetic Preparations

Normal human peripheral blood lymphocytes are prepared by incubation in chromosome-1A media with phytohemagglutinin (Gibco, Grand Island, NY) for 72 h. Where appropriate, 3 mM BrdU is added to the culture 7 h before harvesting to label late-replicating DNA. For metaphase mapping, BrdU enhances chromosome elongation and banding, and enables the direct detection of late-replicating (G) bands using a fluorescein conjugated antibody to BrdU (BMB, Becton Dickinson). For interphase mapping, incorporation of BrdU for this period of time serves to distinguish G1 from S and G2 phase nuclei, which is critical

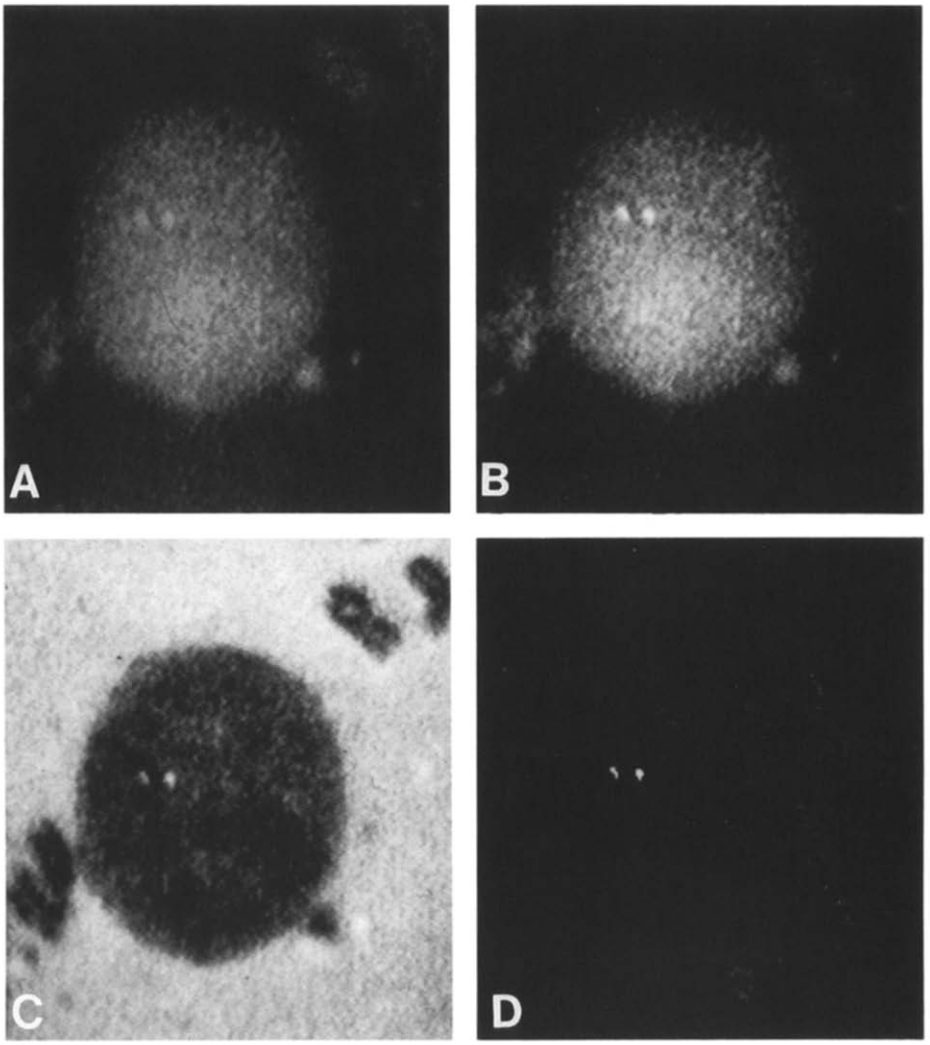

Figure 10. Improvement of marginal signal by processing of a digital image. **A.** A 2-kb probe detected by standard fluorescence microscopy and then photographed using digital imaging microscopy. The two signals represent two copies of the EBV genome in Namalwa cell nuclei. **B.** The same image after application of software for automatic contrast enhancement. Signals can be made even more obvious by more sophisticated processing involving the merging of images captured at different wavelengths (**C**) or the thresholding of values in the display to show only pixels with the highest intensity (**D**).

to the interpretation of signal patterns. Colcemid (0.01 μg/ml) is added 30–90 min prior to fixation. Cells are fixed in 3:1 methanol–acetic acid and dropped on slides according to standard cytogenetic procedures. Cytogenetic slides are air-dried overnight, stored at −80°C, and baked at 65°C for 1–3 h immediately before use.

Probe Preparation

The quality of the probes is extremely important. Biotinated DNA probes are prepared by standard nick translation procedures using biotin–16-dUTP or digoxigenin–11-dUTP (Boehringer Mannheim Biochemicals). We routinely test the level of incorporation of probes using the BRL biotin detection kit to detect a dot blot dilution series on nitrocellulose. Successful detection of 10–25 pg of DNA probe indicates adequate incorporation. The final size of the probe fragments is critical. DNase-I concentration is carefully monitored to provide a range of fragments with a mean length of 200–400 bp, but with none >700 bp in length. Sonicated total human DNA derived from human placenta (0.01–2 mg/ml) (Sigma, St. Louis, MO), preferably, or human Cot-1 DNA (BRL 0.25–0.5 mg/ml), sonicated salmon sperm DNA (0.02 mg/ml) (Sigma) and *Escherichia coli* tRNA (0.02 mg/ml) (BMB) are added after nick translation. Probes are ETOH-precipitated and rinsed in 70% EtOH several times to remove free labeled nucleotides and salt. They are then resuspended in water and stored at 4°C.

For each slide, 50 ng of probe plus an appropriate amount of competitor are lyophilized in an microcentrifuge tube. Slides are denatured in 70% formamide, 2× SSC, at 70°C for 2 min, although other denaturation procedures are also adequate. Time and temperature should be adhered to strictly. Slides are then immersed in 70% EtOH and then dehydrated through 95% and 100% EtOH and air-dried.

Hybridization and Detection

Lyophilized probe is resuspended in 10 μl 100% formamide and denatured at 75°C for 10 min. Ten microliters of hybridization buffer (2 parts autoclaved 50% dextran sulfate, 1 part 10 mg/ml BSA [BMB], 1 part 20× SSC, and 1 part dddH_2O) is mixed into each tube, and the probe is then applied to the slide and covered with a small square of parafilm. Hybridization is at 37°C for a minimum of 3 h; however, we routinely run hybridizations overnight as a matter of convenience. Slides are rinsed 30 min each in 50% formamide 2× SSC, 37°C; 2× SSC, 37°C; and 1× SSC, room temperature. Slides are stained with fluorescein–avidin (10 μg/μl in 4× SSC, 1% BSA) 30–60 min at 37°C and rinsed three times in 4× SSC; 4× SSC/0.05% Triton; and 4× SSC for 10 min each. Anti-BrdU 1:1000, Becton Dickinson, Boehringer Mannheim Biochemicals), and/or antidigoxigenin (1:200, Boehringer Mannheim Biochemicals) can be applied simultaneously with the fluoravidin. Slides are mounted in antibleach media (90% glycerol, 1× PBS, 2.5% DABCO, pH 8.2 [Sigma]) containing either 1 mg/ml DAPI or 5 mg/ml propidium iodide as a fluorescent counterstain. For detection using alkaline phosphatase or other enzymatic reporters, see Garson et al. [46] or Bhatt et al. [94].

We appreciate the contribution of Lisa Marselle to the studies of nuclear RNA. We thank Marie Picard-Craig, Cindy Beaudry, and Laurie Sullivan for their excellent assistance with photographic processing and manuscript preparation and editing.

References

1. Gall JG, Pardue ML: Proc Natl Acad Sci USA 63:378, 1969
2. John H, Birnstiel ML, Jones KW: Nature 223:582, 1969
3. Evans H, Buckland R, Pardue ML: Chromosoma 48:405, 1974
4. Harper ME, Ullrich A, Saunders GR: Proc Natl Acad Sci USA 78:4458, 1981
5. Gerhard DS, Kawasaki ES, Carter Bancroft F, Szabo P: Proc Natl Acad Sci USA 78:3755, 1981
6. Rudkin GT, Stollar BD: Nature 265:472, 1977
7. Manning JE, Hershey ND, Broker TR, Pellegrini M, Mitchell HK, Davidson N: Chromosoma 53:107, 1975
8. Broker TR, Angerer LM, Yen PH, Hershey ND, Davidson N: Nucleic Acid Res 5:363, 1978
9. Bauman JGJ, Wiegant J, Borst P, van Duijn P: Exp Cell Res 128:485, 1980
10. Bauman JGJ, Wiegant J, van Duijn P, et al.: Chromosoma 84:1, 1981
11. Langer PR, Waldrop AA, Ward DC: Proc Natl Acad Sci USA 78:6633, 1981
12. Langer-Safer PR, Levine M, Ward DC: Proc Natl Acad Sci USA 79:4381, 1982
13. Tchen P, Fuchs RPP, Sage E, Leng M: Proc Natl Acad Sci USA 81:3466, 1984
14. Dale RK, Martin E, Livingston DC, Ward DC: Biochemistry 14:2447–2457, 1975
15. Hopman AH, Wiegant J, Tesser GI, van Duijn P: Nucleic Acid Res 14:6471, 1986
16. Verdlov ED, Monastyrskaya GS, Guskava LI, Levitan TL, Scheichenko VI, Budowsky EI: Biophys Acta 340:15, 1974
17. Renz M, Kurz C: Nucleic Acid Res 12:3435, 1984
18. Hamkalo BA: Genet Anal Techn Appl 1991 (in press)
19. Manuelidis L, Langer-Safer PR, Ward DC: J Cell Biol 95:619, 1982
20. Wu W, Davidson N: Proc Natl Acad Sci USA 78:7059, 1981
21. Kress H, Meyerowitz E, Davidson N: Chromosoma 93: 113, 1985
22. Van Prooijen-Knegt AC, van Hoek JFM, Bauman JGJ, van Duijn P, Wool IG, van der Ploeg M: Exp Cell Res 141:397, 1982
23. Albertson D: EMBO J 3:1227, 1984
24. Landegent JE, Jansen in de Wal N, van Ommen G-JB, et al.: Nature 317:175, 1985
25. Albertson DG: EMBO J 4:2493, 1985
26. Lawrence JB, Singer RH: Nucleic Acids Res 13:1777, 1985
27. Singer RH, Lawrence JB, Rashtchian RN: In In situ Hybridization: Application to the Central Nervous System (Valentino K, Eberwine J, Barchas J, eds). New York, Oxford University Press, 1987, pp 71
28. Singer RH, Lawrence JB, Villnave CA: Biotechniques 4:230, 1986
29. Lawrence JB, Villnave CA, Singer RH: Cell 52:51, 1988
30. Singer RH, Ward DC: Proc Natl Acad Sci USA 79:7331, 1982
31. Harper ME, Marselle LM: Can Genet Cytogenet 19:73, 1985
32. Haase AT, Stowring L, Harris JD, et al.: Virology 119: 399–410, 1982
33. Cox KH, DeLeon DV, Angerer LM, Angerer RC: Dev Biol 101:485–502, 1984
34. Manuelidis L: Focus 7:4–8, 1985

35. Lawrence JB, Singer RH, McNeil JA: Science 249:928, 1990
36. Singer RH, Langevin GL, Lawrence JB: J Cell Biol 108:2343, 1989
37. Matsuo T, Heller M, Petti L, O'Shiro E, Kieff E: Science 226:1322, 1984
38. Johnson CV, McNeil JA, Carter KC, Lawrence JB: Genet Anal Techn Appl [in this issue]
39. Nederlof PM, Robinson D, Abuknesha R, et al.: Cytometry 10:20, 1989
40. Pinkel D, Landegent J, Collins C, et al.: Proc Natl Acad Sci USA 85:9138, 1988
41. Lichter P, Cremer T, Tang C-JC, Watkins PC, Manuelidis L, Ward DC: Proc Natl Acad Sci USA 85:9664, 1988
42. Landegent JE, in de Wal NJ, Dirks RW, Baas F, van der Ploeg M: Hum Genet 77:366, 1987
43. Trask B, Pinkel D, van den Engh G: Genomics 5:710, 1989
44. Lichter P, Tang CC, Call K, et al.: Science 247:64, 1990
45. Staunton DE, Fisher RC, LeBeau MM, et al.: J Exp Med 169:1087, 1989
46. Garson JA, van den Berghe JA, Kemshead JT: Nucleic Acids Res 15:4761, 1987
47. Takahashi E, Hori T, Lawrence JB, et al.: Jpn J Hum Genet 34:307, 1989
48. Brown-Shimer S, Johnson KA, Lawrence JB, et al.: Proc Natl Acad Sci USA 87:5148, 1990
49. Viegas-Pequignot E, Dutrillaux B, Magdelenat H, Coppey-Moisan M: Proc Natl Acad Sci USA 86:582, 1989
50. Fan Y-S, Davis LM, Shows TB: Proc Natl Acad Sci USA 87:6223, 1990
51. Davies KE, Pearson PL, Harper PS, et al.: Nucleic Acids Res 11:2303, 1983
52. Hamden DG, Klinger HP (eds): Report of the International Society for Cytogenetic Nomenclature. Basel, Karger, 1985, p 48
53. Lawrence J: In Genome Analysis, vol 1: Genomic and Physical Mapping (Davies K, Tilghman S, eds). Cold Spring Harbor, NY, Cold Spring Harbor Press, 1991
54. Vogel W, Autenreith M, Speit G: Hum Genet 72:129, 1986
55. Manuelidis L, Borden J: Chromosoma 96:397–410, 1988
56. Lichter P, Boyle AL, Cremer T, Ward DC: Genet Anal Techn Appl 8:24–35, 1991
57. Manuelidis L: Proc Natl Acad Sci USA 81:3123, 1984
58. Rykowski MC, Parmelee SJ, Agard DA, Sedat JW: Cell 54:461, 1988
59. Koenig M, Hoffman EP, Bertelsom CJ, Monaco AP, Feener C, Kunkel LM: Cell 50:509, 1987
60. White R, Nakamura Y, O'Connell P, et al.: Genomics 1:364, 1987
61. Lewin B (ed): In Genes II. New York, Wiley, 1985, p 469
62. Paulson JR, Laemmli UK: Cell 12:817, 1977
63. Georgiev GP, Bakayev VV, Nedospason SA, Razir SV, Mantieve VL: Mol Cell Biochem 40:29, 1981
64. Weisbrod S: Nature 297:289, 1982
65. Hamkalo BA, Rattner JB: Q Rev Biol 55:409, 1980
66. Rabl C: Morphologisches Jahrbuch 10:214, 1885
67. Comings D: Am J Hum Genet 20:440, 1968
68. Comings D: Hum Genet 53:131, 1980
69. Agard D, Sedat J: Nature 302:676, 1983
70. Manuelidis L: Hum Genet 71:288, 1985
71. Cremer T, Cremer C, Schneider T, Baumann H, Hens L, Kirsch-Volders M: Hum Genet 62:201, 1982
72. Schardin M, Cremer T, Hager HD, Lang M: Hum Genet 71:281, 1985
73. Hochstrasser M, Mathoy D, Gruenbaum Y, Saumweber H, Sedat JW: J Cell Biol 102:112, 1986
74. Hochstrasser M, Sedat JM: J Cell Biol 104:1455, 1987
75. Hiraoka Y, Minden JS, Swedlow JR, Sedat JW, Agard DA: Nature 342:293, 1989
76. Chung H-MM, Shea C, Fields S, Taub RN, van der Pleog LHT: EMBO J 9:2611, 1990
77. Hutchinson N, Weintraub H: Cell 43:471, 1985
78. Lawrence JB, Singer RH, Marselle LM: Cell 57:493, 1989
79. Xing Y, Lawrence JB: J Cell Biol 112:1055, 1991
80. Lawrence JB, Marselle LM, Byron KS, Sullivan JL, Singer RH: Proc Natl Acad Sci USA 87:5420, 1990
81. Cremer T, Landegent JE, Bruckner H, et al.: Hum Genet 74:346, 1986
82. Pinkel D, Landegent J, Collins C, et al.: Proc Natl Acad Sci USA 85:9138, 1988
83. Tkachuk D, Pinkel D, Kuo WL, Weir U, Gray JW: Genet Anal Techn Appl [this issue]
84. Lux SE, et al.: Nature 345:736, 1990
85. Lawrence JB, Caskey T, McNeil JA: In Miami Short Reports, vol 1: Advances in Gene Technology: The Molecular Biology of Human Genetic Disease (Ahmad F, Bialy H, Black S, eds), Boehringer Mannheim Biochemicals, 1991
86. Hurley EA, Agges S, McNeil JA, et al.: J Virol 1991 (in press)
87. Singer RH, Byron KS, Lawrence JB, Sullivan JL: Blood 74:2295, 1989
88. Pinkel D, Straume T, Gray JW: Proc Natl Acad Sci USA 83:2934, 1986
89. Albertson DG, Fishpool R, Sherrington P, Nacheva E, Milstein C: EMBO J 7:2801, 1988
90. Manuelidis L, Chen TL: Cytometry 11:8, 1990
91. Paddy MR, Belmont AS, Saumweber H, Agard DA, Sedat JW: Cell 62:89, 1990
92. Bauman J, Pinkel D, Trask B, van der Ploeg M, Gray JW (eds): Flow Cytogenetics. New York, Academic Press, 1989, p 275
93. Saez LJ, Gianola KM, McNally EM, et al.: Nucleic Acids Res 15:5443, 1987.
94. Bhatt B, Burns J, Flannery D, McGee OD: Nucleic Acids Res 16:3951, 1988